Virchows Archiv A Pathol Anat (1992) 421:485–490

Virchows Archiv A
Pathological Anatomy and Histopathology

Differential uptake of systemic fluorochrome Hoechst 33342 in lung and liver metastasis of B16 melanoma

Enrique Hilario[1], Emilia Rodeño[1], Josu Simón[1], Francisco J. Alvarez[1], and Salvador F. Aliño[1,2]

[1] Department of Cell Biology and Morphological Sciences, Faculty of Medicine and Dentistry, University of País Vasco, Leioa, Vizcaya, Spain
[2] Department of Pharmacology, Faculty of Medicine, University of Valencia, Blasco Ibanez 15, E-46010 Valencia, Spain

Received May 18, 1992 / Accepted July 20, 1992

Summary. The growth and vascularization patterns of B16 melanoma colonies in the liver and lungs were measured and compared by histological techniques and dye diffusion patterns after injection of the fluorochrome Hoechst 33342. In the liver, the fluorescent pattern of dye diffusion revealed that uninodular tumours measuring up to 146 μm in diameter were not functionally vascularized. However, when the nodules fused to give rise to multinodular tumours measuring between 256 and 366 μm in diameter, a reticular dye diffusion pattern revealed functional tumour vascularization. In the lungs, subpleural, parenchymal and peritubular (i.e. surrounding blood vessels and airways) tumours were observed. The two former classes were vascularized down to thicknesses and diameters of 49 and 24 μm respectively. In contrast, dye diffusion was never seen in peritubular tumour cuffs up to 609 μm in thickness. The results indicate differences in vascularization patterns in B16 tumours in the liver and lungs, and differences between tumours growing in different sites within the lungs. If these results are applicable to metastases in these two organs, they indicate potential diffusion-mediated resistance to chemotherapy, and potential hypoxia-mediated resistance to radiotherapy of both metastases and micrometastases.

Key words: Metastasis – Tumour growth – Tumour vascularization – Fluorescent DNA staining – Fluorochrome diffusion

Introduction

Tumours and metastases present a variable and complex vascular organization (Warren 1979; Suzuki et al. 1984; Weiss et al. 1980; Haugeberg et al. 1988), which differs from that in normal tissues (Suzuki et al. 1984). In addition, Tannock and Steel (1969) have reported that in tumours a significant proportion of blood does not exchange with that of the general circulation, resulting in poorly oxygenated regions with a consequent resistance to radiation, and regions receiving suboptimal doses of chemotherapeutic agents (Tannock 1972; Kennedy et al. 1980; Chaplin et al. 1987).

We have studied the morphology and the functional vascularization of regions of B16 melanoma tumours growing in the lungs and liver, by measuring the diffusion of the fluorochrome Hoechst 33342 injected i.v. into tumour-bearing animals.

Correspondence to: S. F. Aliño

Materials and methods

Mice. Nine to 10-week-old syngeneic male C57BL/6J mice (Iffa-Credo Laboratories, France) were used throughout the study. The experimental procedure was reviewed and accepted by the local ethical committee for animal experimentation. All animal care procedures were performed in accordance with the "Guide for the Care and Use of Laboratory Animals", prepared by the Committee on Care and Use of Laboratory Animals of the Institute of Laboratory Animal Resources, National Research Council, USA (NIH publication no. 86-23).

Cancer cells and culture conditions. B16F10 melanoma cells were maintained in stationary culture in RPMI 1640 medium supplemented with 10% fetal bovine serum (Flow Laboratories, Scotland), at 37° C in a humidified incubator with air plus 5% carbon dioxide. The culture was routinely monitored for mycoplasma contamination. Tumour cells were shaken free after brief exposure to 2 mM EDTA in phosphate-buffered saline (PBS; pH 7.4), and washed once in culture medium without serum and twice with PBS. Cell viability was assessed by trypan blue exclusion, and only single-cell suspensions with greater than 95% viability were used, immediately after washing.

Tumour colony production. Mice were anaesthetized with intraperitoneal injections of pentobarbital (Nembutal; Merck, Darmstadt FRG; 1.2 mg/mouse) in PBS. Lung colonies were obtained by i.v. injection of 10^5 viable B16F10 tumour cells into a lateral tail vein. Liver colonies were produced by intrasplenic injection of 5×10^5 viable B16F10 tumour cells in 0.1 ml of PBS solution (Kopper et al. 1982). Mice were killed after 3, 5 and 7 days. Livers were fixed and processed for transmission electron microscopy, as de-

scribed above. Liver colony growth has been described previously in detail (Aliño and Hilario 1989).

Morphological studies. Seven, 14 and 20 days after tumour cell injection, animals were killed by cervical dislocation. The lungs were perfused by intracardic injection of 1.5% glutaraldehyde in 0.1 M sodium cacodylate/HCl buffer (pH 7.4). Multiple 1 mm^3 pieces were processed for transmission electron microscopy by conventional methods and embedded in Epon 812 (Fluka, Switzerland). Semi-thin sections (1 μm thick), stained with toluidine blue, were evaluated by light microscopy; ultrathin (silver) sections were stained with uranyl acetate and lead citrate, and examined through a Philips EM 300 electron microscope.

Tumour perfusion with Hoechst 33342. Mice with lung colonies received a single tail vein injection of 0.25 ml Hoechst 33342 (1 mg/ml in sterile saline solution; Sigma, St. Louis, Mo., USA) 1 or 10 min before sacrifice (Hilario et al. 1990a).

Mice with liver colonies received a single tail vein injection of 0.25 ml Hoechst 33342, 10 or 20 min before sacrifice (Hilario et al. 1990a).

Lungs and livers were fixed by immersion in liquid nitrogen and, from each organ, a minimum of 12 frozen sections (5 μm thick) were cut 150 μm apart and compared with control sections from non-tumour-bearing mice. Sections were air-dried and observed under ultraviolet light at emission wavelengths in excess of 450 nm.

Assessment of the size of lung and liver metastases. Frozen sections of liver and lungs were projected by means of a Carl Zeiss projection microscope, and the maximum and minimum diameters of randomized non-confluent metastases were measured. To minimize observer bias, all measurements were performed by two observers; the differences were less than 5%.

Liver colonies consisted of either single or several nodules; in both cases, the maximum and the minimum diameters of the tumour foci were recorded. Lung colonies were classified in three morphological groups: parenchymal, subpleural or peritubular, i.e. in rings around the blood vessels and conducting airways. The maximum and the minimum diameters of the parenchymal and subpleural metastases were measured. In peritubular colonies, the thickness of the tumorous rings and the radius of the lumina were measured.

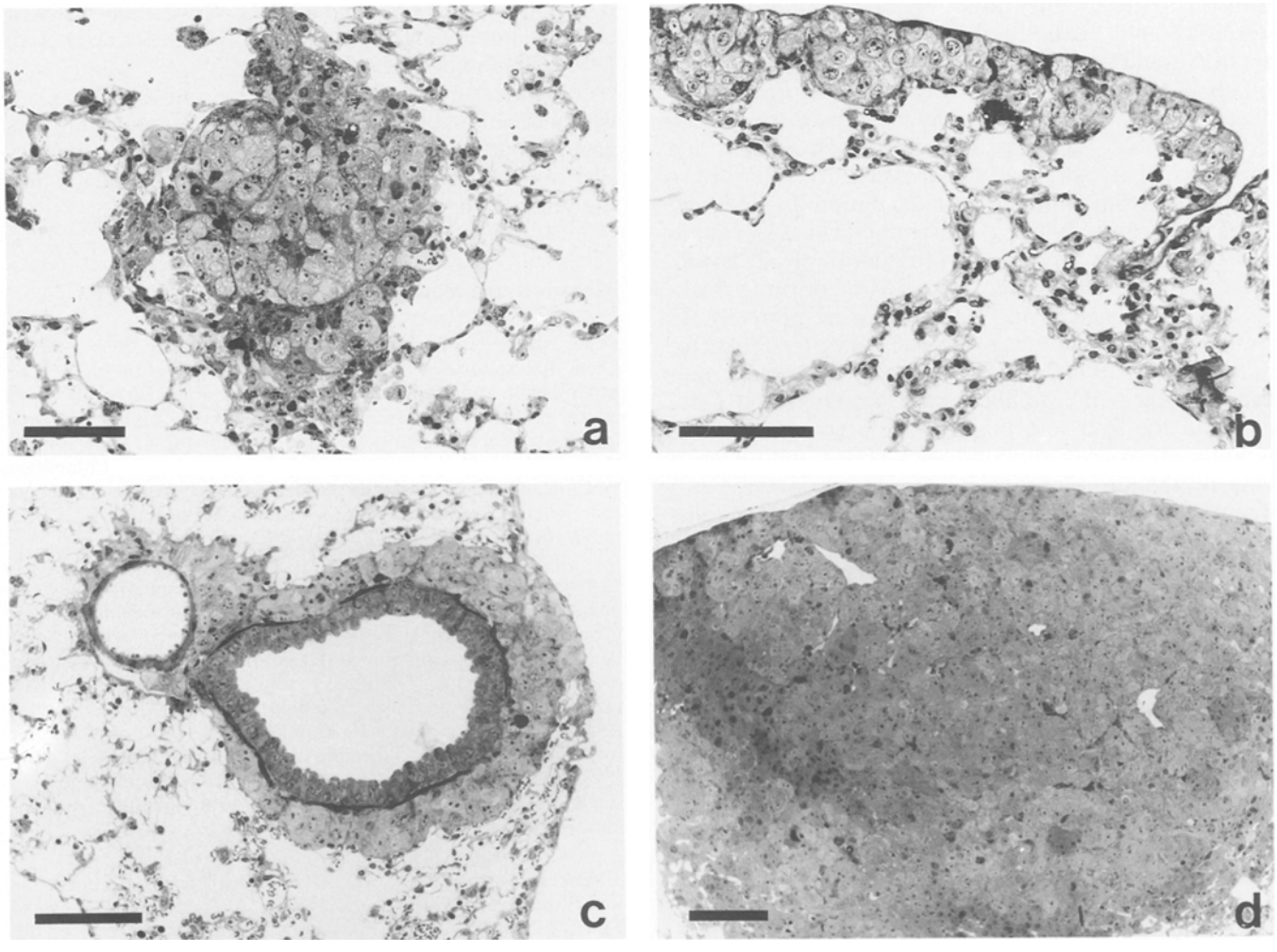

Fig. 1a–d. Semithin sections of B16F10 tumours located in different sites in the lung (*bar* = 100 μm). **a** Solid nodules with poorly defined edges, located in the parenchymal region. **b** Subpleural tumour consisting of several dense nodules, which extend over the subpleural connective tissue giving rise to a flattened lesion. **c** Tumour growing around a blood vessel and airway. **d** Large metastasis showing lost internal nodular organization; only a small number of patent, intratumoral blood vessels can be seen

Results

Morphological study of lung metastasis

Lung tumours in every location grew slowly and thus, 14 days after cancer cell injection, they were pin-points or only detectable by microscopy. These tumours were avascular with scanty interstitial space, and only slight regional variations in morphology and size. Thus, parenchymal lung lesions (< 100 μm diameter) were solid nodules with poorly defined edges (Fig. 1a); subpleural and peritubular foci were flattened, forming subpleural sheets (< 50 μm thickness; Fig. 1b) or rings (< 100 μm ring wall; Figure 1c).

Subsequently, the parenchymal foci fused to form larger single nodules. Subpleural metastases extended over the thin subpleural connective tissue, and sometimes grew down into adjacent alveolar septa giving rise to flat superficial lesions. Peritubular tumours spread over the connective tissue, forming well-developed rings around these structures or entering the alveolar septa; however, the cancer cells usually did not invade the external elastic lamina of the blood vessels, or the muscular layer of the airways. In larger tumours (usually > 300–400 μm), the initial delineation between some of the constituent nodules was lost (Fig. 1d). These tumours consisted of densely packed cancer cells with patent or closed blood vessels; some contained occasional small lacunae lined with cancer cells, and usually containing blood cells.

At the ultrastructural level, cancer cells located in the interstitial connective compartments were in contact with connective tissue elements, pneumocytes and/or endothelial cells, expanding the usually narrow interstitial spaces (Fig. 2a). Cancer cells were also observed inside the lumen of blood vessels, or within the alveolar spaces. During growth the tumours compressed and eventually collapsed most of the alveolar spaces and blood vessels (Fig. 2a, b).

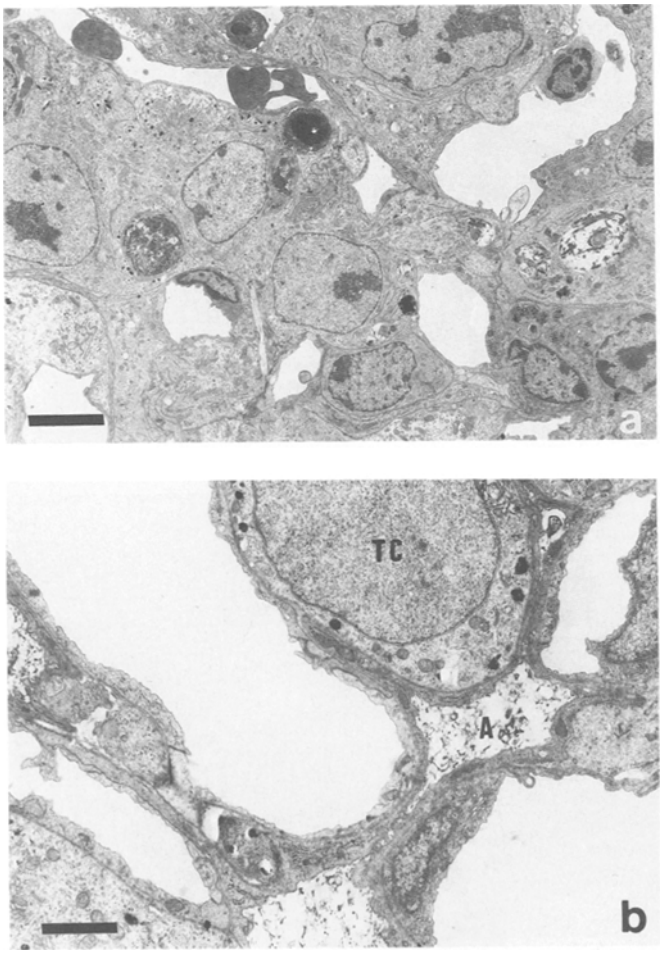

Fig. 2. a Cancer cells invading the interstitial compartment, expanding the usually narrow interstitial spaces. The alveoli are not evident and only blood vessels are observed between tumour cells (*bar* = 5 μm). **b** Early tumour showing alveolar (*A*) compression by tumour cells (*TC*), and electron-dense material filling the alveolar spaces (*bar* = 2 μm)

Tumour size

Liver tumour dimensions are given in Table 1. Although the majority of the uninodular tumours were smaller than the multinodular, some were larger.

Lung tumour dimensions are given in Table 2. Subpleural tumours extended over the subpleural tissue reaching a maximum diameter of 2012 μm, with a maximum depth, into alveolar septa, of 426 μm. This maximum depth of the subpleural tumours fell between the maximal diameters (329 and 548 μm) of parenchymal tumours and in turn was smaller than the thickness of metastases located around blood vessels and conducting airways.

Tumour perfusion study in Hoechst 33342

Following i.v. administration of Hoechst 33342, there is a diffusion-limited delivery of the dye, depending on the proximity of cells to the blood vessels (Loeffler et al. 1987); in tumours, cancer cells close to the blood vessels

Table 1. Size of non-confluent liver B16F10 tumours after 3–7 days

	n	Maximum (D) and minimum (d) diameters (mean ± SE)	Range	Median
Uninodular metastases (3–5 days)	237	D: 145.1 ± 3.7 d: 112.9 ± 2.9	24.3– 304.8 24.3– 243.9	146.3 121.9
Multinodular metastases (7 days)	144	D: 389.4 ± 12.3 d: 285.2 ± 9.1	219.5–1097.5 109.7– 731.7	365.8 256

The number of tumours measured is less than the total number of lesions located in the sections. Tumours were categorized according to whether they consisted of a single nodule or several nodules. In both cases the maximum (D) and the minimum (d) diameters (in micrometres) of whole tumours were measured

Table 2. Size of non-confluent lung B16F10 tumours

	n	Size (mean ± SE)	Range	Median
Parenchymal metastases	143	D: 210.3 ± 8.4 d: 164.0 ± 6.4	48.7– 548.7 36.5– 329.2	195.1 158.5
Subpleural metastases	66	D: 808.5 ± 57.7 d: 169.4 ± 15.5	121.9–2012.1 24.3– 426.8	731.7 158.5
Peritubular metastases	142	R: 134.8 ± 7.9 r: 25.4 ± 1.2	18 – 609 6– 73.1	121.9*,** 24.3

The number of tumours measured is less than the total number of lesions seen in the sections. Tumours are classified according to their parenchymal, subpleural, and peritubular (around blood vessels and conducting airways) location. In parenchymal and subpleural lesions the maximum (D) and the minimum (d) diameters were measured; in peritubular tumours the thickness of the ring or cuff (R) and the lumen radius (r) were recorded in micrometres. Statistical significance from non-parametric Mann-Whitney test of (D + d) parenchymal tumours versus (d) subpleural tumours versus (R) peritubular tumours (*$P < 0.05$); and (d) subpleural tumours versus (R) peritubular tumours (**$P < 0.05$)

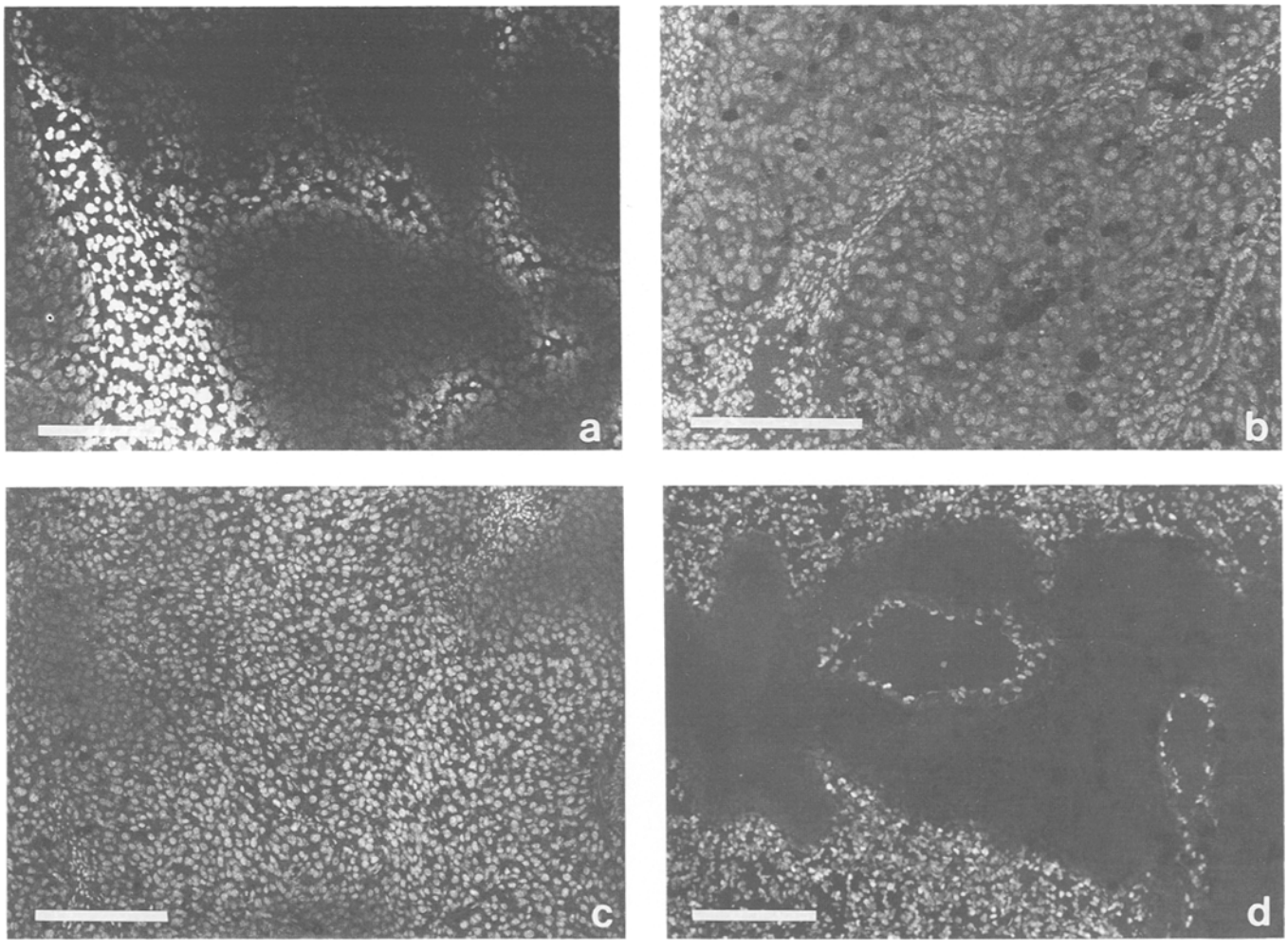

Fig. 3a–d. Fluorescence micrographs of frozen sections of liver and lungs bearing melanoma tumours, 10 min after Hoechst 33342 administration. **a** Liver tumour displaying a reticular fluorescent pattern coincident with the intratumoral blood vessels and delineating the non-fluorescent tumour nodules. **b, c** Lung tumours displaying a diffuse (**b**) or a patchy (**c**) fluorescence, with less intensity than that of the lung cells. **d** Tumour located around a blood vessel showing no detectable fluorescence, in contrast to the endothelium of the blood vessel and lung cells (*bar* = 200 μm)

are brighter than those further away (Chaplin et al. 1985, 1987).

Hoechst 33342 staining of hepatic or pulmonary parenchymal cells was similar in mice bearing metastases and in their respective non-tumour-bearing control groups. Moreover, both in liver and lung tumours similar fluorescent intensity patterns were observed in sections from mice killed 1 and 10 min after dye injection.

Uninodular liver tumours showed no fluorescence, in contrast to "normal" liver cells, which displayed bright fluorescent nuclei. More developed, multinodular tumours showed a reticular fluorescent pattern (Fig. 3a) associated with the intratumoral vascular network. Cancer cells surrounding blood vessels displayed a centrifugally decreasing fluorescence gradient.

In the lung tumours, two different fluorescent patterns were observed in relation to location. Both subpleural and parenchymal foci displayed a diffused (Fig. 3b) or a patchy (Fig. 3c) fluorescent pattern, and the nuclei of cancer cells showed a lesser intensity of fluorescence than the "normal" lung cells. In no case did peritubular lesions display any fluorescence; consequently they were easily identified as shadowy rings in a bright field of "normal" lung cells (Fig. 3d). The cancer cells surrounding the occasional lacunar spaces observed in large metastasis did not display any fluorescence.

Discussion

The liver and lung are common sites for metastasis in many different types of primary cancer. Treatment of hepatic and pulmonary metastases by both chemotherapy and radiation is to some extent regulated by the extent of the functional communications between "normal" and tumour vasculature, which influence both drug delivery and, through tumour oxygenation (hypoxia), radiosensitivity. We describe here the functional blood supply of B16 melanomas seeded in liver and lungs of mice via the bloodstream, at different stages of tumour development.

In the liver, B16 cells are selectively arrested (Hilario et al. 1988) and tumour foci develop (Barberá-Guillem et al. 1989) in the periportal areas of the liver lobule. Initially the tumours are uninodular, but later they fuse to form multinodular lesions. In contrast to the liver, cancer cells arrest and tumour development occurs in all regions of the lung (Dingemans et al. 1985; Orr et al. 1986, 1988; Dingemans 1988; Hilario et al. 1990b), although a preferential subpleural growth has been reported (Dingemans 1988; Orr et al. 1988). In the present study, the development of pulmonary tumours is described in three different sites – subpleural, parenchymal and peritubular – with respect to blood vessels and conducting air passages. The thickness of the flattened subpleural lesions, the diameters of the parenchymal lesions, and the thickness of the peritubular cuffs are all similar and comparable with respect to dye diffusion. Fusion of small lesions was also observed.

The functioning microvasculature of a tumour at any moment may represent only part of its total vascular bed. In vivo estimates of functional microcirculation may therefore give a more meaningful index of the nutritional status of the tissue than methods which identify the total vessel network (Smith et al. 1988). The use of fluorochrome Hoechst 33342 allows the study at the microscopical level of tumour functional vasculature (Smith et al. 1988), as a consequence of its potential for evaluating tissue perfusion (Olive et al. 1985), and therefore as expression of the tumour cell ability to uptake small molecules delivered from the circulation. This results in a situation where tumour cells closest to blood supply become more intensely stained than those further away (Chaplin et al. 1985, 1987; Olive et al. 1985). In the present experiments, dye diffusion was assessed by fluorescence microscopy of frozen sections.

In uninodular liver tumours, with median diameters of 122–146 μm (Table 1), no fluorescence was detected against "normal" background; thus no significant diffusion of a small dye molecule from the host vasculature was recorded. The development of a reticular fluorescence pattern in the larger, multinodular tumours occurred, which indicated vascularization of the peripheries of the individual nodules, when the median diameters of the whole multinodular lesions were in the range of 256–366 μm diameter. These observations are in accord with those reported earlier (Aliño and Hilario 1989).

In lung tumours, parenchymal lesions having diameters of less than 50 μm, and subpleural lesions down to 24 μm thickness, all showed fluorescence above "normal" lung background. In contrast, in none of the peritubular lesions with cuff thicknesses up to 609 μm was fluorescence observed. These observations are in accord with Young et al. (1979), who reported with a different cell line that blood flow varied with the implantation site in the rabbit.

Considerable variations as in perfusion values (Kallinowski et al. 1989), growth rates and extent of avascular regions (Konerding et al. 1989) have been described within the same xenograft line. As a result of a compromised and anisotropic microcirculation, most of these tumours reveal hypoxic and anoxic tissue areas which are already present at early growth stages and expand with tumour growth (Kallinowski et al. 1989; for review see Vaupel et al. 1989).

It is reasonable to expect that the probability of drugs reaching cancer cells within a tumour correlates with dye diffusion, and that cancer cells not taking up the dye would also tend to be radioresistant on account of tissue hypoxia. Of major interest in our present observations is the demonstration that this parameter of functional vascularity effects differs in tumours of the same type growing in the liver and lungs. In addition, small liver tumours and peritubular lung tumours show a degree of functional vascular insufficiency consistent with heightened resistance to chemo- and radiotherapy. However, we must bear in mind that fluorochrome Hoechst 33342 was only used, in the present study, as a tracer of functional vascularization of B16 melanoma metastases. Since cytostatic drugs include a wide variety of

compounds with different physicochemical properties and mechanisms of action, additional studies will be necessary to evaluate the correlation between vascular insufficiency, observed by means of Hoechst 33342, and the tumour cell response to cytostatic drugs.

Acknowledgements. The authors are grateful to Professor Leonard Weiss, Roswell Park Cancer Institute, Buffalo, for his critical comments and help in the preparation of this paper. We are grateful also to Miss C. Otamendi and Mrs. M. Portuondo for technical assistance and to Mrs. M.J. Aldasoro for the preparation of the manuscript. This work was supported by grant UPV/EHU 075.327-16/89 from the University of País Vasco and CICYT PM 900047.

References

Aliño SF, Hilario E (1989) Nodular organization and differential intrametastatic distribution of the fluorescent dye Hoechst 33342 in B16 melanoma liver metastasis. Exp Cell Biol 57:246–256

Barberá-Guillem E, Alonso-Varona A, Vidal-Vanaclocha F (1989) Selective implantation and growth in rats and mice of experimental liver metastasis in acinar zone one. Cancer Res 49:4003–4010

Chaplin DJ, Durand RE, Olive PL (1985) Cell selection from a murine tumour using the fluorescent probe Hoechst 33342. Br J Cancer 51:569–572

Chaplin DJ, Olive PL, Durand RE (1987) Intermittent blood flow in a murine tumor: radiobiological effects. Cancer Res 47:597–601

Dingemans KP (1988) B16 Metastases in mouse liver and lung. II. Morphology. Invasion Metastasis 8:87–102

Dingemans KP, Van Spronsen R, Thunnissen E (1985) B16 melanoma metastases in mouse liver and lung. Invasion Metastasis 5:50–60

Haugeberg G, Strohmeyer T, Lierse W, Bocker W (1988) The vascularization of liver metastasis. Histological investigation of gelatine-injected liver specimens with special regard to the vascularization of micrometastases. J Cancer Res Clin Oncol 144:415–419

Hilario E, Unda F, Aliño SF (1988) Differential distribution of B16F10 melanoma cells in the liver lobule. Exp Cell Biol 56:303–310

Hilario E, Rodeño E, Simón J, Aliño SF (1990a) Identification of intratumoral hematic compartments by a fluorescent dye. Inst Phys Conf Ser 98:731–734

Hilario E, Rodeño E, Simón J, Aliño SF (1990b) Fluorescence and transmission electron microscopy study of the tumour cell implantation in the lung. Trans R Microsc Soc 1:733–736

Kallinowski F, Schlenger KH, Runkel S, et al. (1989) Blood flow, metabolism, cellular microenvironment, and growth rate of human tumor xenografts. Cancer Res 49:3759–3764

Kennedy KA, Teicher BA, Rockwell ST, Sartorelli AC (1980) The hypoxic tumor cell: a target for selective cancer chemotherapy. Biochem Pharmacol 29:1–8

Konerding MA, Steinberg F, Streffer C (1989) The vasculature of xenotransplanted human melanomas and sarcomas on nude mice. Acta Anat 136:21–26

Kopper L, Van Hank T, Lapis K (1982) Experimental model for metastasis formation using Lewis lung tumor. J Cancer Res Clin Oncol 103:31–38

Loeffler DA, Keng PC, Wilson KM, Lord EM (1987) Comparison of fluorescence intensity of Hoechst 33342-stained EMT6 tumour cells and tumour-infiltrating host cells. Br J Cancer 56:571–576

Olive PL, Chaplin DJ, Durand RE (1985) Pharmacokinetics, binding and distribution of Hoechst 33342 in spheroids and murine tumours. Br J Cancer 52:739–746

Orr FW, Adamson IYR, Young L (1986) Quantitation of metastatic tumor growth in bleomycin-injured lungs. Clin Exp Metastasis 4:105–116

Orr FW, Young L, King GM, Adamson IYR (1988) Preferential growth of metastatic tumors at the pleural surface of mouse lung. Clin Exp Metastasis 6:221–232

Smith KA, Hill SA, Begg AC, Denekamp J (1988) Validation of the fluorescent dye Hoechst 33342 as a vascular space marker in tumours. Br J Cancer 57:247–253

Suzuki M, Hori K, Abe I, Saito S, Sato H (1984) Functional characterization of the microcirculation in tumors. Cancer Metastasis Rev 3:115–126

Tannock IF (1972) Oxygen diffusion and the distribution of cellular radiosensitivity in tumours. Br J Radiol 45:515–524

Tannock IF, Steel GG (1969) Quantitative techniques for study of the anatomy and function of small blood vessels in tumors. J Natl Cancer Inst 42:771–782

Vaupel P, Kallinowski F, Okunieff P (1989) Blood flow, oxygen and nutrient supply, and metabolic microenvironment of human tumors: a review. Cancer Res 49:6449–6465

Warren BA (1979) The vascular morphology of tumors. In: Peterson H-I (ed) Tumor blood circulation. CRC Press, Boca Raton, pp 1–47

Weiss L, Haydock K, Pickren JW, Lane WW (1985) Organ vascularity and metastatic frequency. Am J Pathol 101:101–114

Young SW, Hollenberg NK, Abrams HL (1979) The influence of implantation site on tumor growth and blood flow. Eur J Cancer 15:771–777